Entangling Two Individual Atoms of Different Isotopes via Rydberg Blockade

Zeng, Y.; Xu, P.; He, X.; Liu, Y.; Liu, M.; Wang, J.; Papoular, D.J.; Shlyapnikov, G.V.; Zhan, M.

DOI
10.1103/PhysRevLett.119.160502

Publication date
2017

Document Version
Other version

Published in
Physical Review Letters

Entangling two individual atoms of different isotopes via Rydberg blockade: Supplemental Material

Yong Zeng, Peng Xu, Xiaodong He, Yangyang Liu, Min Liu,
Jin Wang, D.J. Papoular, G.V. Shlyapnikov, Mingsheng Zhan
(Dated: September 16, 2017)

I. LASER SYSTEM FOR COHERENT RYDBERG EXCITATIONS

The narrow linewidth and stabilized laser source required to realize a coherent Rydberg excitation are challenging to set up. In our experiment, the Ryd_{480} Ryderg laser is generated from a TA–SHG pro with a seed laser whose wavelength is 960 nm. The frequencies of the lasers Ryd_{480} and Ryd_{780} are locked to a Fabry–Perot cavity with high finesse (58000 for 960 nm and 91000 for 780 nm). We then reduce the linewidth to ∼10 kHz for Ryd_{780} and to ∼20 kHz for Ryd_{480}. The long–term drift of both lasers is less than 50 kHz. The frequency of Ryd_{480} is set to 625253.6 GHz, and we expand the beam waist of Ryd_{480} to $\sim 12.8\,\mu$m, so that it covers both atoms. The Ryd_{780} laser light is divided into two beams with the frequency difference 1127 MHz, corresponding to the difference in the excitation frequencies of ^{85}Rb (Ryd_{780-85}) and ^{87}Rb (Ryd_{780-87}). The frequencies of the Ryd_{780-87} and Ryd_{780-85} lasers are 384223.2GHz and 384224.3 GHz, respectively. The beam waist of Ryd_{780-87} laser is $\sim 7.1\,\mu$m , and Ryd_{780-85} laser has the beam waist of $\sim 7.8\,\mu$m. We use PID controllers with holding function to lock the laser power of Ryd_{480} to 51 mW, and the power of Ryd_{780-87} and Ryd_{780-85} to 5.6 μW. The pulse area fluctuations of the Ryd_{480} and Ryd_{780} laser pulses are suppressed to less than 1%. Using the method from Ref. [1], we estimate $\Omega_{780-87} = 2\pi\cdot$ 226 MHz, $\Omega_{780-87} = 2\pi\cdot$ 206 MHz, and $\Omega_{480-85} = \Omega_{480-87} = 2\pi\cdot$ 28 MHz;

Coherent Rabi oscillations between the ^{87}Rb $|\Uparrow\rangle$ and $|r\rangle$ states and between the ^{85}Rb $|\uparrow\rangle$ and $|r\rangle$ states are shown in Fig. 2b and in Fig. 3b. For ^{87}Rb, the peak–to–peak Rabi amplitude is 0.82 ± 0.02. The survival probability of ^{87}Rb after a π pulse is 13%. This includes the 4% probability of populating the $|\uparrow\rangle$ state, the rest being the result of spontaneous emission from the Rydberg state during the detection. Thus, the Rydberg excitation efficiency for ^{87}Rb is ∼96% and the detection efficiency for the Rydberg state is ∼90%. The corresponding efficiency for ^{85}Rb is almost the same.

II. THE C–NOT GATE AND ENTANGLEMENT FIDELITY

Several reasons limit the heteronuclear C-NOT fidelity in our experiment. They are given in Table 1. The main fidelity loss is due to atom losses (∼0.16), which can be attributed to two reasons. One of them is the imperfect Rydberg excitation and the damping of the Rabi oscillation between the ground and Rydberg states. This can be improved by compensating the stray electric field and by optimizing the powers and frequencies of the excitation lasers [2]. The second reason is the atom loss after the π Rydberg pulses, which is likely due to the mixing of different Rydberg states [3]. It can be improved by controlling the electric field and by using shaped exciting laser pulses [4]. With all these efforts to reduce the atom loss, it is possible to reach a raw fidelity greater than 0.90 in near future. However, in order to reach the error correction threshold of 0.99 for the C-NOT gate, it will take much longer time to carefully address all sources of fidelity loss and to suppress each of them to the level of 0.001.

TABLE I. Error budget for the heteronuclear C–NOT gate fidelity.

Error sources (two qubits)	**Values**
Optical pumping	< 0.01
Atom losses before C–NOT	~ 0.01
Blockade error at $8\,\mu$K	0.03
Spontaneous emission	0.03
Doppler broadening	< 0.01
Total heteronuclear C–NOT error (added in quadrature)	~ 0.05
Background losses (detection, Raman transition)	0.09
Losses due to Rydberg excitation	0.16
Heteronuclear C–NOT fidelity (raw)	0.73
Heteronuclear C–NOT fidelity (corrected for background losses)	0.80
Heteronuclear C–NOT fidelity(corrected for background and excitation losses)	0.95

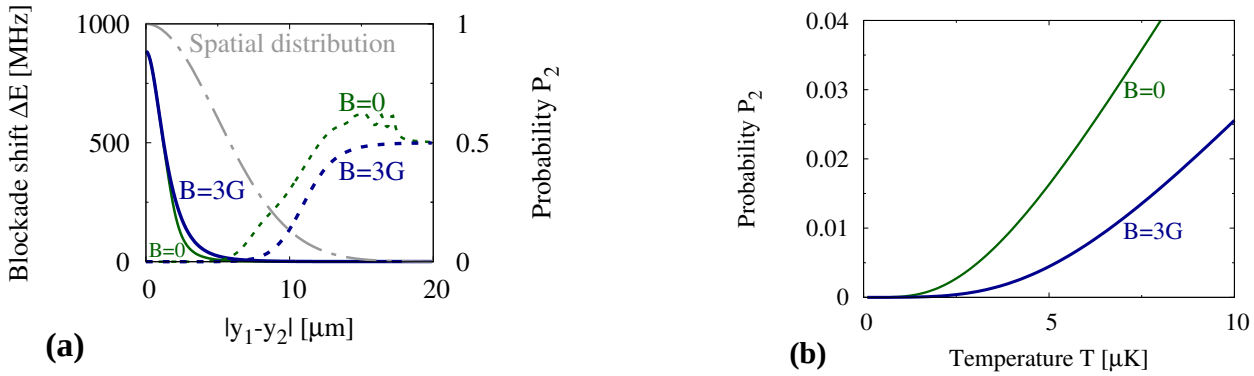

FIG. S1. Calculated heteronuclear Rydberg blockade shift. (a) Double–excitation probability P_{85} (dashed curves, right axis) and the corresponding blockade shift ΔE (solid curves, left axis) as functions of the offset $|y_2 - y_1|$. The spatial probability distribution $p(y = |y_2 - y_1|)$, calculated for $T_{87} = 8\,\mu$K and $T_{85} = 9\,\mu$K, is also shown (gray dashed–dotted curve). (b) Mean double–excitation probability $< P_{85} >$ as a function of the mean temperature T. The thin green curve corresponds to $B = 0$ and the thick blue curve to $B = 3\,$G.

The fidelity of the entangled state is lower than that of the heteronuclear C–NOT gate. This is mainly due to the motion of the ^{87}Rb atom [5]. Single ^{87}Rb atoms accumulate stochastic phases $\Phi = \mathbf{k} \cdot \mathbf{v}\delta t$ during the time δt separating two Rydberg–π pulses. Here, $|\mathbf{k}| = 2\pi/\lambda_{480} - 2\pi/\lambda_{780}$, and $\mathbf{v}$ is the atomic velocity. These phases vary from shot to shot. A simple estimation of the average yields $\langle e^{i\Phi}\rangle = e^{-\langle\Phi^2\rangle/2} = e^{-T|\mathbf{k}|^2\delta t^2/m_{87}}$, where m_{87} is the mass of ^{87}Rb, and we took into account that $\langle \mathbf{v}^2\rangle = 2T/m_{87}$. With $T_{87} = 8\mu K$ and $\delta t = 3.6\mu s$, we find $\langle e^{i\Phi}\rangle = 0.78$, implying a maximum fidelity of $F_{\langle e^{i\Phi}\rangle} = 0.89$. We combine this value with the C–NOT gate fidelity to obtain the maximum entanglement fidelity $F_{\mathrm{ent-max}} = 0.65$. Our experimental result is 0.59 +-0.03, and we attribute the rest of the fidelity loss mainly to the imperfect control of the phase and pulse areas of the Raman $\pi/2$ and π pulses in the "parity analysis" part. Further improvements can be made in the following ways: i) cooling single atoms to 2 μK by adiabatically lowering the trap potential to 0.1 mK; ii) reducing the time separation between two Rydberg π pulses from 3.6 μs to less than 1 μs by increasing the 480nm laser power to about 300 mW; iii) replacing the Raman transition with a microwave transition to improve the accuracy of $\pi/2$ and π pulses. With these improvements, the entanglement fidelity limit by itself can go up from 0.89 to 0.98.

III. CALCULATION OF THE HETERONUCLEAR RYDBERG BLOCKADE SHIFT

We first characterise the Förster resonance yielding the long–range interaction between the control and target atoms. Each atom is assumed to be immobile in its microtrap. If both atoms are excited to Rydberg states with energies close to that of the $79d_{5/2}$ state, their interaction is dominated by the Förster resonance involving the two–atom states in the $(79d_{5/2}, 79d_{5/2})$, $(80p_{3/2}, 78f)$, and $(81p_{3/2}, 77f)$ manifolds. This amounts to restricting the interaction Hamiltonian to a subspace spanned by 436 two–atom states determined by the quantum numbers $|n_a, l_a, j_a, m_a; n_b, l_b, j_b, m_b\rangle$, where the indices a and b refer to ^{87}Rb and ^{85}Rb, respectively. For each atom, m_α gives the projection of $\boldsymbol{j_\alpha}$ along the z axis determined by the static magnetic field. In this basis, the Förster Hamiltonian reads [6]:

$$H_F = V_{\mathrm{dd}} + V_\delta + V_Z \ . \tag{1}$$

The internuclear distance $R \approx 3.8\,\mu$m is much greater than the typical size $n^2 a_0$ of the Rydberg atoms, so that the interaction term in Eq. (1) is the dipole–dipole interaction $V_{\mathrm{dd}} = e^2[\boldsymbol{a}\cdot\boldsymbol{b} - 3(\boldsymbol{a}\cdot\hat{\boldsymbol{R}})(\hat{\boldsymbol{R}}\cdot\boldsymbol{b})]/(4\pi R^3)$, with e being the electron charge and $\hat{\boldsymbol{R}}$ a unit vector along the internuclear separation. The vectors $\boldsymbol{a}$ and $\boldsymbol{b}$ specify the positions of the outermost electron of each atom relative to its nucleus. The diagonal matrix V_δ encodes the Rydberg energy defect of a given basis state with respect to the incident two–atom state $|\mathrm{inc}\rangle$, which is the Zeeman–dressed state related to $|79d_{5/2}, m_a = 5/2; 79d_{5/2}, m_b = 5/2\rangle$ at a vanishing static magnetic field. Finally, the Zeeman term $V_Z = \mu_{\mathrm{B}} B_{\mathrm{stat}} \sum_{\alpha=a,b}(g_l l_{\alpha z} + g_s s_{\alpha z})$ describes the interaction of each atom with the static magnetic field B_{stat}, with $l_{\alpha z}$ and $s_{\alpha z}$ being the components of $\boldsymbol{l}$ and $\boldsymbol{s}$ along the z axis, and g_l and g_s the corresponding g–factors. Like in the numerical analysis of Ref. [1], the Hamiltonian H_F accounts for the Zeeman mixing of single–atom states with different j, and for the mixing of single–atom states with different m due to the angle between z and $\hat{\boldsymbol{R}}$.

We now calculate the probability for both atoms to be in an excited Rydberg state, and the corresponding blockade shift ΔE, for fixed control and target atoms. Initially, the control atom is in the dressed Rydberg state $|r\rangle$ and the target atom is in the ground hyperfine state $|\Uparrow\rangle$, so that the atom pair undergoes oscillations in between the state $|r\Uparrow\rangle$ and the doubly–excited Förster states. We write the Hamiltonian governing these oscillations as a block matrix:

$$H = \begin{pmatrix} 0 & W \\ W^\dagger & H_F - E_{\rm inc} \end{pmatrix} \quad \text{with} \quad W^\dagger = \frac{\hbar\Omega_{85}}{2} |{\rm inc}><r\Uparrow| \ , \tag{2}$$

where H_F is the Förster Hamiltonian of Eq. (1), $E_{\rm inc}$ is the energy of the incident Förster state $|{\rm inc}\rangle$, and W represents the Rabi coupling in between the states $|\Uparrow\rangle$ and $|r\rangle$ of ^{85}Rb. For a given offset $y = |y_2 - y_1|$, the double–excitation probability then reads $P_{85}(y,t) = 1 - |\langle r\Uparrow| e^{-iHt/\hbar} |r\Uparrow\rangle|^2$, where t is the duration of the Rydberg pulse on ^{85}Rb. Here, $P_{85}(y,t)$ represents the total probability for the atom pair to be in any one of the 436 two–atom Rydberg states involved in the Förster resonance. The probability $P_{85}(y,t)$ rapidly oscillates as a function of time, and our numerical results for the time–averaged $P_{85}(y)$ are shown in Fig. S1a along with the corresponding blockade shift $\Delta E(y) = \hbar\Omega_{87}(1/P_{85}(y) - 1)^{1/2}$. We find very strong blockade shifts $\Delta E/h \gtrsim 600\,{\rm MHz}$ for offsets $y < 1\mu$m. The blockade shift decreases with increasing y and is of the order of a few MHz for $y \sim 10\,\mu$m.

Finally, we evaluate the role of the thermal broadening of the spatial probability distribution for the atoms. For the relatively high temperatures of our experiment the motion of the atoms is classical, and the probability density for finding $y_2 - y_1 = y$ is a Gaussian, $p(y) = e^{-y^2/2\sigma^2}/[\sigma(2\pi)^{1/2}]$. The standard deviation σ satisfies the relation $\sigma^2 = k_B T/(m_{\rm red}\omega_y^2)$, where ω_y is the trapping frequency along the y direction for both microtraps, the reduced mass is $m_{\rm red} = m_{87}m_{85}/(m_{87} + m_{85})$, and the mean temperature T satisfies the relation $T/m_{\rm red} = T_{87}/m_{87} + T_{85}/m_{85}$. The temperatures and the trapping frequencies enter our model only through the combination T/ω_y^2, which characterises the spatial extent of the classical motion of the atoms along y. We calculate the mean double–excitation probability $< P_{85} >= \int p(y)P_{85}(y)dy$ and plot this quantity as a function of the mean temperature T in Fig. S1b. In our experiment, $T_{87} = 8\,\mu$K, $T_{85} = 9\,\mu$K, and $\omega_y/2\pi = 1.39\,$kHz, yielding an average double–excitation probability $< P_{85} >\approx 0.013$. This is of the same order of magnitude as the observed quench of the Rabi oscillation amplitude shown in Fig. 3b.

Our results for $\Delta E(y)$ for offsets $y \lesssim 1\,\mu$m are two orders of magnitude larger than the corresponding prediction of Ref. [1], because our experiment explores a different regime for the Förster resonance. Indeed, the typical Rydberg energy defect, $h \times 200\,$MHz, is smaller than the dipole–dipole interaction which is of the order of $(n^2 a_0 e)^2/4\pi\epsilon_0 R^3 = h\times 700\,$MHz for $R = 3.8\mu$m. Therefore, the Förster energies scale with $1/R^3$ as in Ref. [7] (whereas they scale with $1/R^6$ for the parameters of Ref. [1]). Then, the order of magnitude of the blockade shift ΔE is $V_{\rm dd}^2/\sqrt{V_{\rm dd}^2 + (\hbar\delta)^2} \approx V_{\rm dd}$, in accordance with the small–y results in Fig. S1a.

For the temperatures of our experiment the system explores larger values of the offset y and, hence, larger values of R with a non–negligible probability (namely, both are of the order of 10μm). Then, the dipole–dipole interaction is smaller than the Rydberg energy defect, yielding Förster energies that decay as $1/R^6$ and, hence, a much weaker Rydberg blockade.

[1] E. Urban, T. A. Johnson, T. Henage, L. Isenhower, D. D. Yavuz, T. G. Walker, and M. Saffman, Observation of Rydberg blockade between two atoms. *Nat. Phys.* **5**, 110 (2009).

[2] A. Browaeys, D. Barredo and T. Lahaye, Experimental investigations of dipole–dipole interactions between a few Rydberg atoms. *J. Phys. B: At. Mol. Opt. Phys.* **49**, 152001 (2016).

[3] K. M. Maller, M. T. Lichtman, T. Xia, Y. Sun, M. J. Piotrowicz, A. W. Carr, L. Isenhower, and M. Saffman, Rydberg-blockade controlled-not gate and entanglement in a two-dimensional array of neutral-atom qubits.*Phys. Rev. A* **92**, 022336 (2015).

[4] L. S. Theis, F. Motzoi, F. K. Wilhelm, and M. Saffman, High-fidelity Rydberg-blockade entangling gate using shaped, analytic pulses. *Phys. Rev. A* **94**, 032306 (2016).

[5] T. Wilk, A. Gaetan, C. Evellin, J. Wolters, Y. Miroshnychenko, P. Grangier, and A. Browaeys, Entanglement of two individual neutral atoms using Rydberg blockade. *Phys. Rev. Lett.* **104**, 010502 (2010).

[6] M. Saffman, T. G. Walker, and K. Mølmer, Quantum information with Rydberg atoms. *Rev. Mod. Phys.* **82**, 2313 (2010).

[7] A. Gaetan, Y. Miroshnychenko, T. Wilk, A. Chotia, M. Viteau, D. Comparat, P. Pillet, A. Browaeys, and P. Grangier, Observation of collective excitation of two individual atoms in the Rydberg blockade regime. *Nat. Phys.* **5**, 115 (2009).